Analytical theory of external cavity modes of a semiconductor laser with phase conjugate feedback

T. Erneux[a], A. Gavrielides[b], K. Green[c] and B. Krauskopf[d]
[a]Université Libre de Bruxelles, Optique Nonlinéaire Théorique, Campus Plaine, C.P. 231, 1050 Bruxelles, Belgium
[b]Nonlinear Optics Group, Air Force Research Laboratory, 3550 Aberdeen Ave. SE, Kirtland AFB, NM 87117-5776, USA
[c]Department of Computer Science, KU Leuven, Celestijnenlaan 200A, 3001 Heverlee, Belgium
[d]Department of Engineering Mathematics, University of Bristol, Bristol BS8 1TR, United Kingdom

ABSTRACT

The rate equations describing a laser with phase conjugate feedback are analyzed in the case of non-zero detuning. For low feedback rates and detuning, the stability diagram of the steady state is similar to the laser subject to injection. A stable steady state may loose its stability through a Hopf bifurcation exhibiting a frequency close to the relaxation oscillation frequency of the solitary laser. We also construct time-periodic pulsating intensity solutions exhibiting frequencies close to an integer multiple of the external cavity frequency. These solutions have been found numerically for the zero detuning case and play an important role in the bifurcation diagram.

1 INTRODUCTION

Semiconductor lasers that exhibit narrow linewidth of the order of a few kilohertz are important in applications such as communication and spectroscopy. One of the most efficient methods to reduce the linewidth of diode lasers is to use optical feedback to stabilize the frequency of the laser and to additionally reduce the linewidth from several tens of megahertz to tens of kilohertz[1–3] . The most common method to implement optical feedback is to redirect a portion of the outcoupled light back into the cavity by an external mirror or a grating[2] . This technique takes advantage of the extreme sensitivity of the laser diode to even minute optical feedback and to the length of the external delay. However, this scheme requires to control precisely the feedback phase in order to maintain the minimum linewidth, and to reduce the low frequency noise. Both these deleterious effects can be completely removed by the use of phase conjugate feedback from a phase conjugate mirror[4,5] . Several such experiments have shown that using phase conjugate feedback indeed leads to a stabilization of the laser frequency and dramatic narrowing of the linewidth. However, as the strength of the feedback is increased undesired instabilities are also induced[6–8] .

The effects of phase conjugate feedback (PCF) versus conventional optical feedback (COF) were explored by Kürz and Mukai[8] for a specific experimental configuration. The phase conjugator used in this experiment was a broad area laser and was based on spatially nondegenerate four wave mixing. The advantages of the setup were that the response time of the conjugator was limited only by the carrier lifetime (a few nanoseconds) and the spatial four wave mixing configuration allowed for the separation of the pump, probe, and signal beam in the far field. Regardless of the feedback intensity, stable operation could not be achieved in the conventional case, where an active stabilization of the external cavity length to suppress mode hopping would be needed. For the phase conjugate case, a sharp resonance peak at 32.7 MHz and harmonics of this frequency were observed. The linewidth of the central mode was 25 kHz and was observed for hours with no stabilization of the external cavity length.

As already mentioned, the PCF laser is no more stable for larger values of the feedback strength. Several studies of the laser rate equations have been undertaken. Earlier results were obtained by numerical simulations[9,17–19] or simplified linear stability analyses[12,13] . By taking advantage of recent numerical continuation methods, stable and unstable steady and periodic solutions were computed as a function of the feedback strength. These techniques allowed more systematic bifurcation studies[22–24] in terms of one or two parameters. In particular, Green and Krauskopf[24] found that stable branches of time-periodic intensities sequentially appear between domains of chaotic dynamics. Because the intensity oscillates at a frequency close to an integer multiple of the external cavity frequency, these regimes have been called external-cavity modes (ECMs) by analogy to the ECMs of the COF laser. More recently, analytical techniques have been developed in order to construct these ECMs and their validity have been tested by comparing bifurcation diagrams[26] . For the simplest case of zero detuning, the laser field is a combination of two modes of the form

$$Y \simeq A_1 \exp(i\omega t) + A_2 \exp(-i\omega t) \tag{1}$$

where A_1, A_2 are two complex amplitudes. Numerical bifurcation studies are so far limited to the case of zero detuning. The purpose of this paper is to show that an extension of the analytical approach is possible and that some effects of the detuning can be highlighted.

The paper is organized as follows. In Section 2, we formulate the PCF laser equations and determine the basic steady states. In Section 3, we investigate the Hopf bifurcation for low feedback rate and obtain a stability diagram that is similar to the laser subject to an injected signal. In Section 4, we construct an approximation of the ECM pulsating intensity solutions which appear as isolated branches in the bifurcation diagram.

2 DIMENSIONLESS EQUATIONS

e start with the PCF rate equations in dimensionless form. This formulation is briefly described in Appendix A. For analytical simplicity, we neglect nonlinear gain saturation. The phase-conjugate mirror is located at distance $L = c\tau/2$ from the laser. We assume that it operates through four-wave mixing in a Kerr-type nonlinear medium with femtosecond response. In the case of nearly degenerate FWM, a small mismatch is present between the frequencies of signal and pump waves i.e., $\omega_s = \omega_p + \Delta$. Since the phase-conjugate frequency is $\omega_c = \omega_p - \Delta$, the reflected and incident waves differ by 2Δ in frequencies. The PCF equations for the complex laser field Y and the carrier density Z are then given by

$$\frac{dY}{dt} = Z(1+i\alpha)Y + \gamma Y^*(t-\theta)\exp\left(2i\Delta(t-\theta/2) + i\phi_0\right), \tag{2}$$

$$T\frac{dZ}{dt} = P - Z - (1+2Z)\left|Y\right|^2. \quad (3)$$

In these equations, α is the linewidth enhancement factor, γ is the dimensionless feedback rate, $\theta \equiv \tau/\tau_p$ is the external cavity round trip time normalized by the photon lifetime, $T \equiv \tau_e/\tau_p$ is the ratio of the carrier and photon lifetimes, P is the pump parameter above threshold, Δ is the frequency detuning, and ϕ_0 is a phase shift acquired in the phase-conjugate mirror.

Eqs. (2)-(3) admits a simple steady state solution of the form

$$Y = A\exp(i\Delta t + i\frac{\phi_0}{2}) \text{ and } Z = C. \quad (4)$$

We called this solution a steady state because the intensity $\left|Y\right|^2$ is steady. Inserting (4) into Eqs. (2)-(3) leads to the following conditions for A and C

$$i\Delta A = C(1+i\alpha)A + \gamma A^*, \quad (5)$$
$$0 = P - C - (1+2C)AA^*. \quad (6)$$

Eq. (5) is a homogeneous equation for A and A^*. It admits a nontrivial solution only if C satisfies the following quadratic equation

$$\gamma^2 = C^2 + (\alpha C - \Delta)^2. \quad (7)$$

Knowing C, we then determine $\left|A\right|^2$ from Eq. (6) as

$$\left|A\right|^2 = \frac{P-C}{1+2C} \geq 0. \quad (8)$$

Eq. (7) describes two branches of solutions emerging from a limit point (saddle-node bifurcation or SN). Steady state locking occurs if

$$\gamma \geq \frac{|\Delta|}{\sqrt{1+\alpha^2}}. \quad (9)$$

3 HOPF BIFURCATION AT LOW FEEDBACK RATE

The conditions for a Hopf bifurcation are given by Eqs. (53) and (54) in Appendix B. C and σ represent the steady state amplitude of Z and the frequency of the oscillations at the Hopf bifurcation point, respectively. These equations are transcendental equations which are difficult to solve. Our analysis differs from previous attempts to determine approximations of the Hopf bifurcation points[9,14,10] by the application of asymptotic techniques[15] . Specifically, we take advantage of the large value of T and look for an approximation for C and σ valid in the limit T large. To this end, we introduce a small parameter ε defined by

$$\varepsilon \equiv T^{-1} \quad (10)$$

and scale C and σ with respect to ε. We also need to specify the scalings of the other laser parameters since distinguish limits of the Hopf conditions are possible.

The simplest approximation is based on the idea that for low feedback rates, the frequency at the Hopf bifurcation must be close to the laser relaxation frequency defined by[16]

$$\sigma_R \equiv (2\varepsilon P)^{1/2}. \quad (11)$$

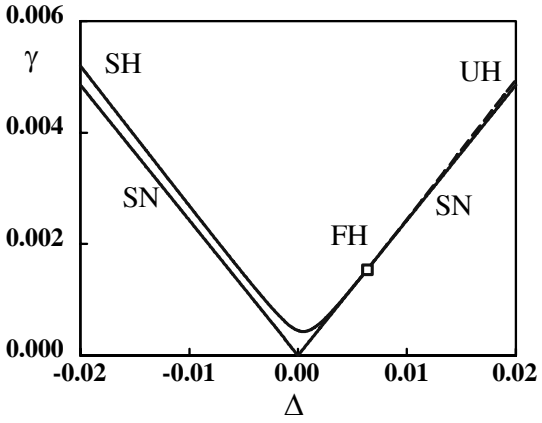

Figure 1: SN and Hopf bifurcations. The two SN lines mark the transition to steady state locking as we progressively increase γ from zero. The full SH and broken UH lines correspond to Hopf bifurcation points from a stable and an unstable steady state, respectively. The codimension two bifurcation point FH (Fold-Hopf) is the intersection of the SN and Hopf curves. It is characterized by one zero eigenvalue and a pair of purely imaginary eigenvalues. The values of the parameters are $\alpha = 4$, $P = 1$, $T = \theta = 1000$.

Assuming the scalings

$$C = O(\varepsilon),\ \sigma = O(\varepsilon^{1/2}),\ P = 0(1),\ \Delta = O(\varepsilon) \text{ and } \theta = O(\varepsilon^{-1}), \tag{12}$$

we collect the leading terms in Eqs. (53) and (54). We obtain

$$\sigma^3 - 2\varepsilon P\sigma = 0, \tag{13}$$

$$-2\sigma^2 C + \varepsilon(1+2P)\sigma^2 + 2\varepsilon P(C + (C\alpha - \Delta)\alpha)(\cos(\sigma\theta) + 1) = 0. \tag{14}$$

From (13), we find that $\sigma = \sigma_R$ where σ_R is defined by (11). From (14), we determine C as

$$C = \frac{\varepsilon(1+2P) - \Delta\alpha(\cos(\sigma\theta)+1)}{[2-(1+\alpha^2)(\cos(\sigma\theta)+1)]}. \tag{15}$$

The expression (15) is valid provided the denominator is not too small, i.e., if $\cos^2(\sigma\theta/2) \neq (1+\alpha^2)^{-1}$. Finally, we compute γ using (7). Fig. 1 shows the SN bifurcation and Hopf bifurcation points in parameter space (Δ, γ). The stability boundaries are similar to the curves previously shown[12,13] and recall the stability diagram of a laser subject to injection (see Discussion). The SN point is characterized by a single zero eigenvalue. At this point emerge a branch of stable steady states and a branch of unstable steady states (saddle points). From an analysis of the characteristic equation in the limit of small real eigenvalues, we find that the stable (unstable) steady states satisfy the condition

$$C < \frac{\Delta}{1+\alpha^2}\ (C > \frac{\Delta}{1+\alpha^2}). \tag{16}$$

Other Hopf bifurcation points can be determined analytically assuming different scalings for C and σ[26]
.

4 EXTERNAL CAVITY MODES

We next concentrate on the pulsating intensity solutions called ECMs. These solutions differ from the Hopf bifurcation solutions by the fact that they exhibit oscillating frequencies that are comparable to the external cavity frequency. They do not emerge from the steady state but sequentially appear as isolated branches of solutions[24,26] . As in the previous section, we may take advantage of the large value of T and seek an asymptotic solution. This time we assume that the basic time is not $\sigma_R t$ but t.

4.1 Asymptotic solution

The technique was first developed for the COF laser[20] and then applied for the PCF problem with zero detuning[26] . Specifically, we seek a solution of Eqs. (2) and (3) of the form

$$Y = Y_0(t) + \varepsilon Y_1(t) + ... \tag{17}$$
$$Z = Z_0(t) + \varepsilon Z_1(t) + ... \tag{18}$$

where ε is defined by (10). Introducing (17) and (18) into Eqs. (2) and (3) and equating to zero the coefficients of each power of ε leads to a sequence of linear problems to solve. The equations for Y_0 and Z_0 are given by

$$Y_0' = (1+i\alpha)Z_0 Y_0 + \gamma Y_0^*(t-\theta)\exp\left(i2\Delta(t-\theta/2)+i\phi_0\right), \tag{19}$$
$$Z_0' = 0. \tag{20}$$

Eq. (20) implies that

$$Z_0 = C \tag{21}$$

is a unknown constant. C now represents the leading approximation for $Z(t)$. Eq. (19) with (21) is then linear and admits a solution of the form

$$Y_0 = \exp(i\frac{\phi_0}{2})\left[A_1\exp(i\omega_1 t) + A_2\exp(i\omega_2 t)\right] \tag{22}$$

provided that ω_1 and ω_2 verify the resonance condition

$$\omega_2 + \omega_1 = 2\Delta \tag{23}$$

and that A_1 and A_2 satisfy the following homogeneous system of equations

$$i\omega_1 A_1 = C(1+i\alpha)A_1 + \gamma A_2^*\exp\left[i(-\Delta\theta+\omega_2\theta)\right], \tag{24}$$
$$i\omega_2 A_2 = C(1+i\alpha)A_2 + \gamma A_1^*\exp\left[i(-\Delta\theta+\omega_1\theta)\right]. \tag{25}$$

The condition (23) implies that (22) can be rewritten as

$$Y_0 = \exp(i\Delta t + i\frac{\phi_0}{2})\left[A_1\exp(i(\omega_1-\Delta)t) + A_2\exp(-i(\omega_1-\Delta)t)\right]. \tag{26}$$

Knowing A_1 and A_2, the intensity of the laser field then is

$$|Y|^2 \simeq |A_1|^2 + |A_2|^2 + 2|A_1||A_2|\cos\left(2(\omega_1-\Delta)t+\psi\right) \tag{27}$$

which displays the frequency

$$\omega = 2|\omega_1 - \Delta|. \tag{28}$$

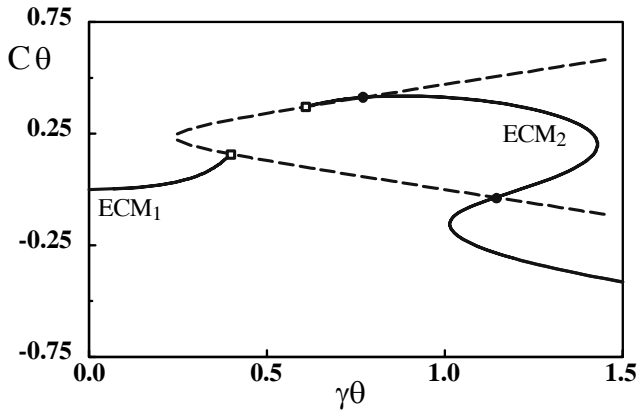

Figure 2: Bifurcation diagram of the ECMs. The full and broken lines correspond to the ECMs and steady states, respectively. Squares denote points where ω_1 equals Δ implying a zero frequency for the ECMs. Dots mark points where steady and ECMs admit the same Z in first approximation but not the same intensities. The values of the parameters are the same as in Figure 2 and $\Delta\theta = 1$.

4.2 Solution of the bifurcation equations

Eqs. (24) and (25) are the bifurcation equations for A_1 and A_2. From (25), we determine A_2 as

$$A_2 = \frac{\gamma A_1^* \exp\left[i(-\Delta\theta + \omega_1\theta)\right]}{i\omega_2 - C(1+i\alpha)}. \tag{29}$$

Substituting (29) into Eq. (24), we find

$$i\omega_1 A_1 - C(1+i\alpha)A_1 = \gamma^2 \frac{A_1 \exp\left[i(-\omega_1+\omega_2)\theta\right]}{-i\omega_2 - C(1-i\alpha)}. \tag{30}$$

Assuming $|A_1| \neq 0$, Eq. (30) implies

$$\left[i\omega_1 - C(1+i\alpha)\right]\left[-i\omega_2 - C(1-i\alpha)\right] = \gamma^2 \exp\left[i(-\omega_1+\omega_2)\theta\right], \tag{31}$$

or equivalently, from the real and imaginary parts:

$$\omega_1\omega_2 - C\alpha(\omega_2+\omega_1) + C^2(1+\alpha^2) = \gamma^2 \cos\left[(-\omega_1+\omega_2)\theta\right], \tag{32}$$

$$C(\omega_2 - \omega_1) = \gamma^2 \sin\left[(-\omega_1+\omega_2)\theta\right]. \tag{33}$$

Using (23), we may eliminate ω_2 and obtain

$$\omega_1(2\Delta - \omega_1) - 2C\alpha\Delta + C^2(1+\alpha^2) = \gamma^2 \cos\left[2(\Delta-\omega_1)\theta\right], \tag{34}$$

$$2C(\Delta - \omega_1) = \gamma^2 \sin\left[2(\Delta-\omega_1)\theta\right]. \tag{35}$$

From (35), we get

$$C = \frac{\gamma^2 \sin\left[2(\Delta-\omega_1)\theta\right]}{2(\Delta-\omega_1)} \tag{36}$$

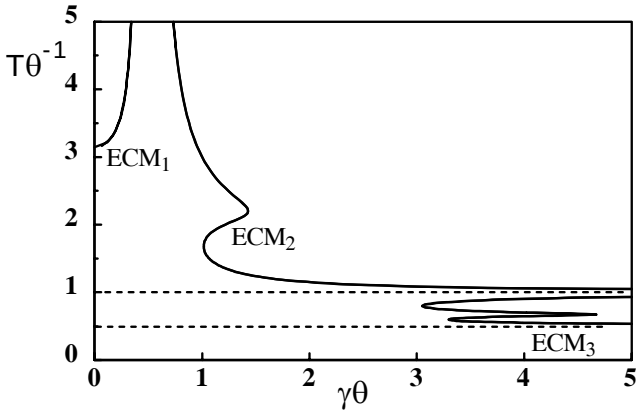

Figure 3: Succesive ECMs. The first ECM emerges from $\gamma = 0$ at $\mathrm{T}\theta^{-1} = \pi/\Delta\theta = \pi$ since $\Delta\theta = 1$. The next ECMs admit a limit as $\gamma\theta \to \infty$ given by $\mathrm{T}\theta^{-1} = 1/(n-1)$ $(n = 2, 3, ...)$.

and

$$\omega_1(2\Delta - \omega_1) - \frac{\gamma^2 \sin\left[2(\Delta - \omega_1)\theta\right]}{(\Delta - \omega_1)}\alpha\Delta$$
$$+\frac{\gamma^4 \sin^2\left[2(\Delta - \omega_1)\theta\right]}{4(\Delta - \omega_1)^2}(1 + \alpha^2) = \gamma^2 \cos\left[2(\Delta - \omega_1)\theta\right]. \tag{37}$$

We may solve these equations in the following way. For a fixed Δ, we continuously change ω_1 and determine γ^2 from the quadratic equation (37). We then obtain C from (36). See Figure 2. In order to determine the intensity, we need a second relation between A_2 and A_1. This relation is obtained by applying a solvability condition for the Z_1 equation[26] (not shown).

In Fig. 3, we represent the period of the intensity oscillations defined as

$$\mathrm{T} \equiv 2\pi/\omega = \pi/\left|\Delta - \omega_1\right|. \tag{38}$$

The first ECM solution emerges from $\gamma = 0$ ($C = 0$, $\omega_1 = 2\Delta$) with a period $\mathrm{T} = \pi/\Delta$ i.e.e, controlled by the detuning. The period then quickly increases to infinity as the ECM branch approaches the steady state. The next ECM branches all exhibit a limit as $\gamma\theta \to \infty$ which is given by

$$\mathrm{T} \to \theta/(n-1) \text{ as } \gamma\theta \to \infty \tag{39}$$

for $n = 2, 3, ...$

5 DISCUSSION

We have examined the laser PCF equations with non zero detuning and determined two type of solutions. First, we obtain an approximation of the first Hopf bifurcation point for low feedback rate and detuning and found a stability diagram similar to the diagram of the laser subject to an injected

signal[27] . In the latter case, the steady state locking condition for low γ is the same as (9) but not the Hopf bifurcation condition. For the injection laser, the Hopf bifurcation appears as $Z = C$ where

$$C = \frac{1}{\alpha^2 - 1} \left[-\varepsilon(1 + 2P) + \Delta\alpha \right]. \tag{40}$$

This expression matches (15) for the PCF laser only if $\cos(\sigma_R \theta) = 0$. There is thus an effect of the delay even for low feedback rate. Second, we investigate a particular class of solutions where the laser field is a linear combination of two time-periodic modes, in first approximation. As investigated in detail for the zero detuning case[26] , these solutions called external cavity modes (ECMs) of the PCF laser seem to organize the bifurcation diagram by sequentially appearing with distinct periods as we increase the feedback rate. In the nonzero detuning case, we note that the first ECM emerges from $\gamma = 0$ and connects the steady state branch.

6 ACKNOWLEDGMENTS

The research was supported by the Fonds National de la Recherche Scientifique (Belgium) and the InterUniversity Attraction Pole program of the Belgian government.

7 APPENDIX A. DIMENSIONLESS PCF EQUATIONS

The laser rate equations are

$$\frac{dE}{dt'} = \frac{1}{2} \left[(G_N(N - N_0) - \tau_p^{-1})(1 + i\alpha) \right] E + \kappa E^*(t' - \tau) \exp(2i\delta(t' - \tau/2) + i\phi_0), \tag{41}$$

$$\frac{dN}{dt'} = \frac{I}{q} - \frac{N}{\tau_e} - G_N(N - N_0) \left| E \right|^2. \tag{42}$$

Introducing the new variables t, Y and Z defined by

$$t \equiv t'/\tau_p,\ Y \equiv \sqrt{\frac{\tau_e G_N}{2}} E \text{ and } Z \equiv \frac{G_N \tau_p}{2}(N - N_{sol}), \tag{43}$$

into Eqs. (41) and (42) and find

$$\begin{aligned} \frac{dY}{dt} &= (1 + i\alpha) Y Z + \gamma Y^*(t - \theta) \exp(2i\Delta(t - \theta/2) + i\phi_0), \\ T\frac{dZ}{dt} &= P - Z - (1 + 2Z) \left| Y \right|^2. \end{aligned} \tag{44}$$

where

$$\gamma = \kappa\tau_p,\ \theta = \tau/\tau_p,\ T = \tau_e \tau_p^{-1},\ \Delta = \delta\tau_p, \tag{45}$$

$$I_{th} = \frac{N_{sol} q}{\tau_e},\ P = \frac{G_N \tau_p \tau_e}{2}\left(\frac{I - I_{th}}{q}\right). \tag{46}$$

8 STEADY STATE AND HOPF BIFURCATION CONDITIONS

Introducing the decomposition

$$Y = R\exp(i\Delta t + i\phi) \tag{47}$$

into Eqs. (2) and (3), we obtain the following three equations for R, ϕ, and Z

$$\begin{aligned} R' &= ZR + \gamma R(t-\theta)\cos(\phi + \phi(t-\theta) - \phi_0), & (48)\\ \phi' &= -\Delta + \alpha Z - \gamma\frac{R(t-\theta)}{R}\sin(\phi + \phi(t-\theta) - \phi_0), & (49)\\ Z' &= \varepsilon\left[P - Z - (1+2Z)R^2\right]. & (50) \end{aligned}$$

The steady state solution satisfies the conditions $R' = \phi' = Z' = 0$. From the steady state equations, we firs determine an equation for ϕ given by

$$\Delta = -\gamma\left[\alpha\cos(2\phi - \phi_0) + \sin(2\phi - \phi_0)\right] \tag{51}$$

and Z and R^2 are related to ϕ as

$$Z = C = -\gamma\cos(2\phi - \phi_0),\ R^2 = \frac{P-C}{1+2C} > 0. \tag{52}$$

Note the simple relation between γ and C given by (7). Since there are two branches of steady states, it will be mathematically more convenient to use C as our bifurcation parameter. From the linearized equations, we determine the characteristic equation for the growth rate λ of a small perturbation. A Hopf bifurcation is possible if λ is purely imaginary. Introducing $\lambda = i\sigma$ into the characteristic equation, we obtain from the real and imaginary parts two equations for C and σ given by:

$$\begin{aligned} 0 &= \sigma\left[(C^2 + (\alpha C - \Delta)^2)(\cos(2\sigma\theta) - 1) + \sigma^2\right]\\ &\quad +\varepsilon\frac{1+2P}{1+2C}\left[-(C^2 + (\alpha C - \Delta)^2)\sin(2\sigma\theta) + 2\sigma C\right]\\ &\quad +2\varepsilon(P-C)\left[-(C + (\alpha C - \Delta)\alpha)\sin(\sigma\theta) - \sigma\right], \end{aligned} \tag{53}$$

$$\begin{aligned} 0 &= \sigma\left[(C^2 + (\alpha C - \Delta)^2)\sin(2\sigma\theta) - 2\sigma C\right]\\ &\quad +\varepsilon\frac{1+2P}{1+2C}\left[(C^2 + (\alpha C - \Delta)^2)(\cos(2\sigma\theta) - 1) + \sigma^2\right]\\ &\quad +2\varepsilon(P-C)(C + (\alpha C - \Delta)\alpha)(\cos(\sigma\theta) + 1) \end{aligned} \tag{54}$$

where ε is defined by (10).

9 REFERENCES

[1] R. Lang and K. Kobayashi, IEEE J. Quant. Electron. **QE-16**, 347 (1980)

[2] R. W. Tkach and A. R. Chraplyvy, J. Lightwave Technol. **LT-4**, 1665 (1986)

[3] R. Wyatt and W. J. Delvin, Electron. Lett. **19**, 110 (1983)

[4] K. Vahala, K. Kyuma, A. Yariv, S.-K. Kwong, M. Cronin-Colomb, and K. Y. Lau, App. Phys. Lett. **49**, 1563 (1986)

[5] M. Ohtsu, I. Koshiishi, and Y. Teramachi, Jpn. J. App. Phsy. **29**, L2060 (1990)

[6] B. W. Liby, and D. Statman, IEEE Trans. of Quant. Electron. **32**, 835 (1996)

[7] A. Shiratori, and M. Obara, Appl. Phys. Lett. **69**, 1515 (1996)

[8] P. Kürz, and T. Mukai, Opt. Lett. **21**, 1369 (1996)

[9] D.H. DeTienne, G.R. Gray, G.P. Agrawal, and D. Lenstra, IEEE J. of Quant. Electron. **33**, 838 (1997)

[10] W.A. van der Graaf, Nonlinear Dynamics of Semiconductor Lasers Driven by External Optical Fields, Ph.D. Thesis Vrije Universiteit Amsterdam (1997)

[11] W.A. van der Graaf, L. Pesquera, and D. Lenstra, in "Physics and Simulations of Optoelectronic Devices VI", W.W. Chow, M. Osinski, Eds., SPIE Proc. **3283**, 522 (1998)

[12] W.A. van der Graaf, L. Pesquera, and D. Lenstra, Opt. Lett. **23**, 256 (1998)

[13] G.H.M. van Tartwijk, H.J.C. van der Linden, and D. Lenstra, Opt. Letters **17**, 1590 (1992)

[14] A. Murakami, J. Ohtsubo and Y. Liu, IEEE J. of Quantum Electronics **33**, 1825 (1997)

[15] C.M. Bender and S.A. Orszag, "Advanced Mathematical Methods for Scientists and Engineers", Mc Graw Hill, New York (1978)

[16] T. Erneux, in "Physics and Simulations of Optoelectronic Devices VIII", R. Binder, P. Blood, M. Osinski, Eds., Proc. SPIE **3944**, 588 (2000)

[17] G.R. Gray, D. Huang, and G.P. Agrawal, Phys. Rev. A **49**, 2096 (1994)

[18] B. Krauskopf, G.R. Gray, and D. Lenstra, in "Physics and Simulations of Optoelectronic Devices VI",W.W. Chow, M. Osinski, Eds., SPIE Proc. **3283**, 510 (1998)

[19] B. Krauskopf, G.R. Gray, and D. Lenstra, Phys. Rev. E **58**, 7190 (1998)

[20] T. Erneux, F. Rogister, A. Gavrielides, and V. Kovanis, Opt. Comm. **183**, 467 (2000)

[21] B. Krauskopf and K. Green, in "Physics and Simulations of Optoelectronic Devices X", P. Blood, M. Osinski, Y. Arakawa, Eds., Proc. SPIE **4646**, 453 (2002)

[22] K. Green and B. Krauskopf, Phys. Rev. E **66**, 016220 (2002)

[23] K. Green, B. Krauskopf, and K. Engelborghs, Physica D **173**, 114 (2002)

[24] K. Green and B. Krauskopf, Int. J. Bifurcation and Chaos **13**, 2589 (2003)

[25] K. Green, B. Krauskopf, and G. Samaey, SIAM J. Appl. Dyn. Syst. **2**, 254 (2003)

[26] T. Erneux, A. Gavrielides, K. Green and B. Krauskopf, Phys. Rev. E **68**, 066205 (2003)

[27] A. Gavrielides, V. Kovanis, T. Erneux, Opt. Comm. **136**, 253 (1997)